

# The synthesis, and molecular and electronic structure of dodecacarbonyl( $\mu_4$ - $\eta^2$ -prop-1-ene-1,1-diyl)tetrairon, $\text{Fe}_4(\text{CO})_{12}(\mu_4\text{-}\eta^2\text{-C}=\text{CHCH}_3)^\dagger$

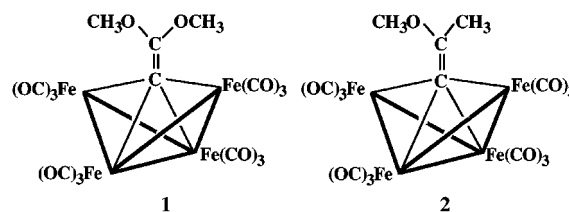
John S. Bradley,\*<sup>‡</sup> Suzanne Harris\*<sup>§</sup> and Ernestine W. Hill

Exxon Research and Engineering Company, Rt 22E, Annandale, NJ 08801, USA

The  $\mu_4$ -vinylidene cluster  $\text{Fe}_4(\text{CO})_{12}(\mu_4\text{-}\eta^2\text{-C}=\text{CHCH}_3)$  has been prepared by the sequential reaction of  $\text{Fe}_4(\text{CO})_{12}[\text{C}=\text{C}(\text{CH}_3)(\text{OCH}_3)]$ , with lithium triethylhydroborate and trimethylsilyl trifluoromethanesulfonate. The cluster has an open butterfly arrangement of four iron atoms with the prop-1-ene-1,1-diyl ligand bound to all four iron atoms in a manner giving an axial C=C bond, perpendicular to both the mutually perpendicular Fe–Fe vectors between the wingtip iron atoms ( $\text{Fe}_w$ ) and between the hinge iron atoms ( $\text{Fe}_h$ ). The vinylidene carbon atom lies below the  $\text{Fe}_w\text{--Fe}_w$  vector, essentially inside the  $\text{Fe}_4$  core. Molecular orbital calculations using the Fenske–Hall method were carried out for the cluster, showing that the geometry of the  $\text{Fe}_4\text{C}=\text{CHCH}_3$  fragment results from overlap between the formal C=C double bond and the two  $\text{Fe}_w$  iron atoms. Comparisons are drawn between  $\text{Fe}_4(\text{CO})_{12}(\mu_4\text{-}\eta^2\text{-C}=\text{CHCH}_3)$  and other  $\text{Fe}_4$  vinylidene clusters.

Correlations between the structures and spectroscopic properties of organometallic cluster molecules have often been used to provide comparative data for surface studies of adsorbed organic molecules on catalytically important metal surfaces, and in at least this sense the often cited analogy between molecular clusters and surfaces can be of considerable utility. It can be the case, however, that ostensibly similar organic species can bind to apparently similar cluster frameworks in quite different manners, and the factors affecting this variation are not often apparent. If the use of organometallic analogs as a guide to the probable structures of organic species on surfaces is to have value, such differences must be explored and explained.

The substituted ethenediyl fragment,  $\text{C}=\text{CR}^1\text{R}^2$  (referred to as vinylidene throughout the text), is known to bind between the wings of butterfly tetranuclear metal clusters, or to similarly shaped clefts in larger clusters, in a  $\mu_4\text{-}\eta^2$  geometry, but two different bonding modes are possible. The majority of clusters in this class display a bent geometry in which the vinylidene carbon is bound to all four metal atoms, but the vinyl carbon is bound to only one of the wingtip metal atoms, leaning away from the other.<sup>1–10</sup> In the second class, of which only two examples, both  $\text{Fe}_4$  butterfly clusters, are known for tetranuclear clusters,<sup>11</sup> the vinylidene fragment is bound symmetrically to both the wingtip metal atoms, and projects essentially perpendicular to the two orthogonal Fe–Fe vectors in the  $\text{Fe}_4$  butterfly core. A similar symmetric binding geometry has been observed for a vinylidene fragment bound in an  $\text{FeRu}_3$  butterfly cleft in an  $\text{FeRu}_5$  cluster.<sup>12</sup> The structures of the two  $\mu_4$ -vinylidene tetrairon butterfly clusters,  $\text{Fe}_4(\text{CO})_{12}[\text{C}=\text{C}(\text{OCH}_3)_2]$  **1** and  $\text{Fe}_4(\text{CO})_{12}[\text{C}=\text{C}(\text{CH}_3)(\text{OCH}_3)]$  **2**, which were prepared by the methylation of the corresponding clusters  $[\text{Fe}_4(\text{CO})_{12}\{\text{CC}(\text{O})(\text{OCH}_3)\}]^-$  and  $[\text{Fe}_4(\text{CO})_{12}\{\text{CC}(\text{O})\text{CH}_3\}]^-$  respectively,<sup>13</sup> can be rationalised in terms of the interaction between the vinylidene carbon orbitals and the  $\text{Fe}_4\text{C}$  core.<sup>11</sup> This interaction was strongly affected by the presence of the one or two electron donating methoxy groups at the vinyl carbons. In this



paper we report the synthesis and structure of a third tetrairon vinylidene cluster,  $\text{Fe}_4(\text{CO})_{12}(\text{C}=\text{CHCH}_3)$  **3**, in which the absence of an electron donating group at the vinyl carbon atom results in a marked departure from the structures of the two previously reported analogs **1** and **2** in that the vinylidene carbon is situated *below* the vector between the two wingtip iron atoms in **3**, but *above* this vector in **1** and **2**. This difference is analysed in terms of the electronic structures of the three clusters **1**, **2** and **3**. A significant similarity in the structures of these three vinylidene clusters is that in each the vinylidene group is axial [*i.e.* perpendicular both to the vector between the wingtip iron ( $\text{Fe}_w$ ) atoms and to that between the hinge iron ( $\text{Fe}_h$ ) atoms] with respect to the cluster core.

## Results and Discussion

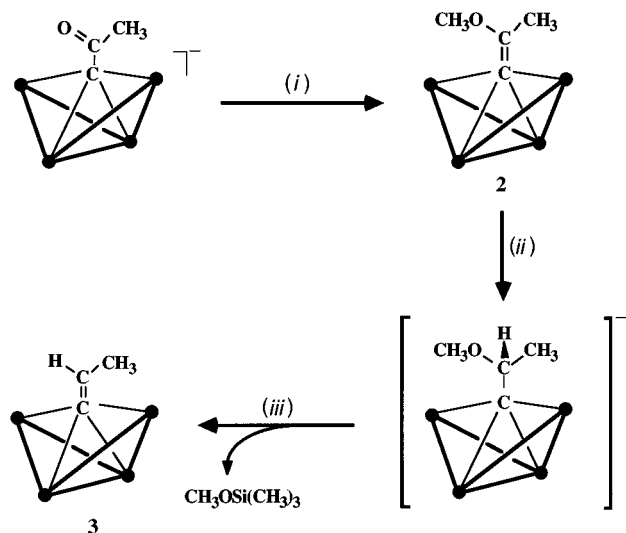
The complex  $\text{Fe}_4(\text{CO})_{12}[\text{C}=\text{C}(\text{CH}_3)(\text{OCH}_3)]$  **2**<sup>11</sup> served as the precursor for the synthesis of **3** by sequential hydride addition to the vinyl carbon and demethoxylation of the resulting cluster anion (Scheme 1). Lithium triethylhydroborate reacts in thf at  $-80^\circ\text{C}$  with **2** to give a dark green intermediate, whose IR spectrum at this temperature (2000s, 1974  $\text{cm}^{-1}$ ) is consistent with its formulation as  $[\text{Fe}_4(\text{CO})_{12}\{\mu_4\text{-CCH}(\text{CH}_3)(\text{OCH}_3)\}]^-$  by comparison with the IR spectra of other  $[\text{Fe}_4(\text{CO})_{12}(\mu_4\text{-CR})]^-$  clusters.<sup>13</sup> Trimethylsilyl trifluoromethanesulfonate, a versatile reagent in organic synthesis which has been used in demethoxylation of organic<sup>14</sup> and organometallic compounds,<sup>15</sup> reacts readily with the intermediate anion with the loss of methoxide as trimethylsilyl ether, yielding  $\text{Fe}_4(\text{CO})_{12}(\text{C}=\text{CHCH}_3)$  **3** in moderate yield.

The IR spectrum of **3** comprises, in addition to carbonyl absorptions at 2098w, 2058s, 2030s, 1980  $\text{cm}^{-1}$ , two bands at 1457 and 1373  $\text{cm}^{-1}$ . These we assign to coupled vibrational modes associated with the  $\nu(\text{C}=\text{C})$  and  $\delta(=\text{CH})$  modes of the  $\text{C}=\text{CH}(\text{CH}_3)$  group, by analogy with similar assignments made

<sup>†</sup> Dedicated to the memory of Professor Sir Geoffrey Wilkinson.

<sup>‡</sup> Present address: Max-Planck-Institut für Kohlenforschung, Kaiser-Wilhelm-Platz 1, D45470 Mülheim an der Ruhr, Germany.

<sup>§</sup> Present address: Department of Chemistry, University of Wyoming, Laramie 82071, USA.



**Scheme 1** (i)  $\text{Me}_3\text{O}^+\text{BF}_4^-$ ,  $\text{CH}_2\text{Cl}_2$ ; (ii)  $\text{Li}^+\text{Et}_3\text{BH}_4^-$ , tetrahydrofuran (thf),  $-80^\circ\text{C}$ ; (iii)  $\text{F}_3\text{CSO}_3\text{Si}(\text{CH}_3)_3$

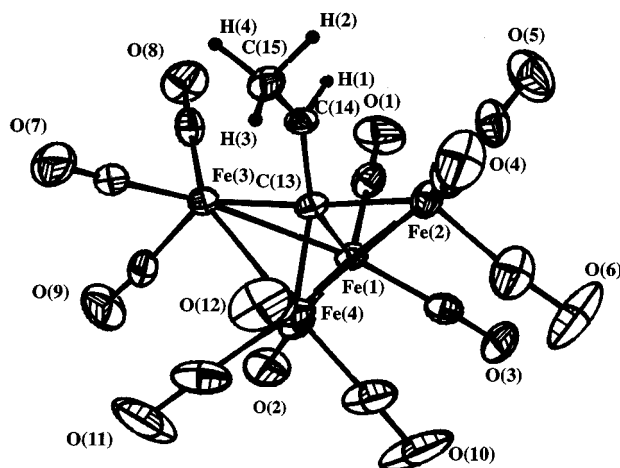


**Fig. 1** An ORTEP<sup>17</sup> drawing of  $\text{Fe}_4(\text{CO})_{12}(\mu_4\text{-}\eta^2\text{-C=CHCH}_3)$  **3** showing 50% probability thermal ellipsoids. Only oxygen atoms for the carbonyls are numbered, and these define the carbon atom numbering scheme. Hydrogen atoms are depicted as spheres of arbitrary radius. The dihedral angle between the two wings [ $\text{Fe}(1)\text{-Fe}(2)\text{-Fe}(4)$  and  $\text{Fe}(1)\text{-Fe}(3)\text{-Fe}(4)$ ] of the cluster is  $104^\circ$

for bands at  $1467$  and  $1328\text{ cm}^{-1}$  in the IR spectrum of  $\text{H}_2\text{Os}_3(\text{CO})_9(\text{C}=\text{CH}_2)$ .<sup>16</sup>

The  $^{13}\text{C}$  NMR spectrum of **3** at  $28^\circ\text{C}$  is consistent with the orientation of the  $\mu_4\text{-C}=\text{CHCH}_3$  group such that the  $\text{C}(\text{H})\text{CH}_3$  group lies in the plane defined by the two 'hinge' iron atoms and the vinylidene carbon, similar to that found for the vinylidene groups in  $\text{Fe}_4(\text{CO})_{12}[\text{C}=\text{C}(\text{OCH}_3)_2]$  **1** and  $\text{Fe}_4(\text{CO})_{12}[\text{C}=\text{C}(\text{CH}_3)(\text{OCH}_3)]$  **2**, whose structures we reported earlier.<sup>11</sup> Two low-field resonances of equal intensity at  $\delta$  213.5 and 213.1 are assigned to the two sets of three equivalent carbonyl ligands on freely rotating  $\text{Fe}(\text{CO})_3$  groups on the 'hinge' of the cluster core, which are inequivalent due to the asymmetry of the  $\text{C}=\text{CHCH}_3$  group. The single resonance at  $\delta$  206.8 is assigned to the six equivalent CO ligands in the freely rotating  $\text{Fe}(\text{CO})_3$  groups on the 'wingtips' of the cluster core.

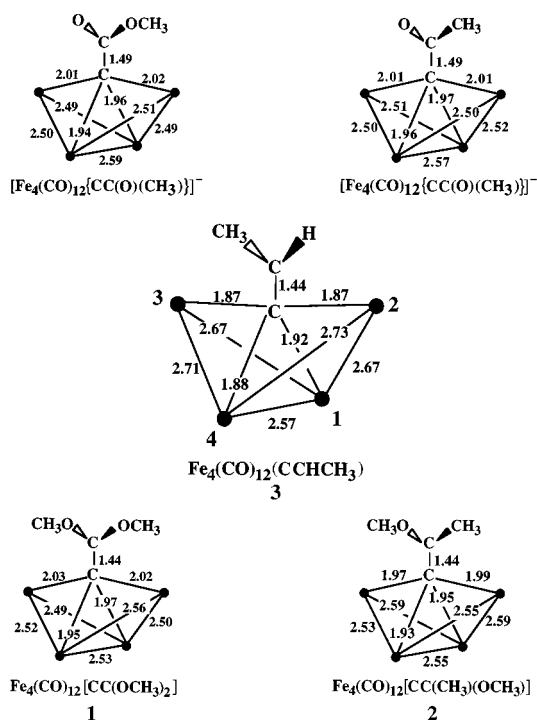
The structure of **3** as determined by X-ray crystallography comprises four iron atoms arranged in a butterfly configuration, each bearing three carbonyl ligands, as is found for other molecules with the  $[\text{Fe}_4(\text{CO})_{12}\text{C}]$  core stoichiometry. The numbering scheme, shown in Fig. 1, assigns  $\text{Fe}(4)$  and  $\text{Fe}(1)$  to the hinge iron atoms *syn* and *anti* with respect to the vinylidene methyl group. The three carbonyl ligands on  $\text{Fe}(4)$  are rotated slightly from an eclipsed configuration with respect to the corresponding ligands on  $\text{Fe}(1)$  in a manner dictated by the

non-bonding interaction between the vinylidene methyl group and  $\text{CO}(12)$  on  $\text{Fe}(4)$ . The  $\text{Fe-Fe}$  vectors between the wingtip iron atoms  $\text{Fe}(1)$  and  $\text{Fe}(4)$  and the hinge iron atoms  $\text{Fe}(2)$  and  $\text{Fe}(3)$  are slightly longer for  $\text{Fe}(4)\text{-Fe}(2)\text{-Fe}(3)$  ( $2.72 \pm 0.01\text{ \AA}$ ) than for  $\text{Fe}(1)\text{-Fe}(2)\text{-Fe}(3)$  ( $2.67\text{ \AA}$ ), and the hinge  $\text{Fe-Fe}$  vector  $\text{Fe}(1)\text{-Fe}(4)$  is markedly shorter than either at  $2.54\text{ \AA}$ . The dihedral angle between the two triangular wings of the butterfly  $\text{Fe}(1)\text{-Fe}(2)\text{-Fe}(4)$  and  $\text{Fe}(1)\text{-Fe}(3)\text{-Fe}(4)$  is  $104^\circ$ . The  $\mu_4\text{-C}=\text{CHCH}_3$  group is bound in an approximately axially symmetrical fashion, with the  $\text{C}=\text{C}$  vector  $\text{C}(13)\text{-C}(14)$  perpendicular to the  $\text{Fe}(2)\text{-Fe}(3)$  vector [ $\text{Fe}(3)\text{-C}(13)\text{-C}(14) = \text{Fe}(2)\text{-C}(13)\text{-C}(14) = 88.0(3)^\circ$ ]. The vinylidene group is tilted slightly out of a perfectly axially symmetric orientation, in the  $\text{Fe}(1)\text{C}(13)\text{Fe}(4)$  plane, with  $\text{Fe}(1)\text{-C}(13)\text{-C}(14) = 133.4(3)^\circ$ , and  $\text{Fe}(4)\text{-C}(13)\text{-C}(14) = 142.5(3)^\circ$ , presumably reflecting the non-bonding repulsive interaction between the vinylidene methyl group  $\text{C}(15)\text{H}_3$  and  $\text{CO}(12)$ , the proximal carbonyl ligand on  $\text{Fe}(4)$ . A similar distortion was found for the analogous  $\text{C}=\text{C}(\text{CH}_3)(\text{OCH}_3)$  group in **2**, and was ascribed to just such a steric repulsion which differentiated between the methoxy group and the sterically more demanding methyl group.<sup>11</sup> By tilting in this manner, the vinylidene carbon  $\text{C}(13)$  in fact moves slightly off the  $\text{Fe}(2)\text{-Fe}(3)$  vector, and towards  $\text{Fe}(4)$ , [ $\text{Fe}(1)\text{-C}(13) = 1.922(6)$ ,  $\text{Fe}(4)\text{-C}(13) = 1.875(6)\text{ \AA}$ ], while  $\text{C}(14)$  is displaced slightly to the other side [ $\text{Fe}(1)\text{-C}(13)\text{-C}(14) = 133.4(3)$ ,  $\text{Fe}(4)\text{-C}(13)\text{-C}(14) = 142.5(3)^\circ$ ]. Perhaps the most interesting aspect of the structure of **3** is the fact that the vinylidene carbon  $\text{C}(13)$  lies *below* the  $\text{Fe}(2)\text{-Fe}(3)$  vector, and  $\text{C}(14)$  is thus brought to within  $2.32\text{ \AA}$  of the wingtip iron atoms  $\text{Fe}(2)\text{-Fe}(3)$ . This structural feature will be discussed in terms of the electronic structure of **3** below. The vinylidene carbon-carbon bond  $\text{C}(13)\text{-C}(14)$  is  $1.44\text{ \AA}$  in length.

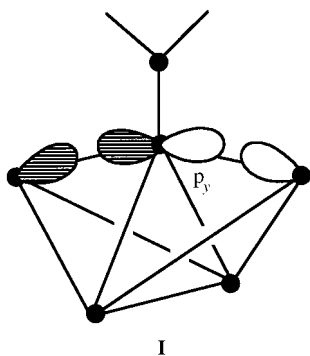
The structure of **3** is particularly interesting when seen in comparison with the two previously reported  $\text{Fe}_4$ -vinylidene clusters,  $\text{Fe}_4(\text{CO})_{12}[\text{C}=\text{C}(\text{OCH}_3)_2]$  **1** and  $\text{Fe}_4(\text{CO})_{12}[\text{C}=\text{C}(\text{CH}_3)(\text{OCH}_3)]$  **2** (the precursor to **3**), and it is instructive to make these comparisons in the context of a progression in increasing C-C bond order in a series from the formally singly bonded methylidyne clusters  $[\text{Fe}_4(\text{CO})_{12}\{\text{CC}(\text{O})(\text{OCH}_3)\}]^-$  and  $[\text{Fe}_4(\text{CO})_{12}\{\text{CC}(\text{O})(\text{CH}_3)\}]^-$  (which are the precursors to **1** and **2**), through the methoxy-substituted vinylidene clusters **1** and **2**, to the formally doubly bonded prop-1-ene-1,1-diyl cluster **3**.

The structures of **1**, **2** and **3** are shown schematically in Scheme 2, together with the structures of the anionic precursors (referred to as methylidyne throughout the text). In **1** and **2**, the  $\mu_4$ -vinylidene carbons lie well above the vector between the wingtip iron atoms, giving rise to an  $\text{Fe}(2)\text{-C-Fe}(3)$  angle of  $149.5^\circ$  in **1** and  $157.7^\circ$  in **2**. In **3** the vinylidene carbon lies *below* the  $\text{Fe}(2)\text{-Fe}(3)$  vector giving an  $\text{Fe}(2)\text{-C}(13)\text{-Fe}(3)$  angle in **3** of  $173.4(3)^\circ$ . This difference is seen also in a comparison of the dihedral angles between the two triangular wings of the  $\text{Fe}_4$  butterflies for the three vinylidene clusters. The dihedral angles are  $127^\circ$  in **1**,  $122^\circ$  in **2** and  $104^\circ$  in **3**. The  $\text{Fe}_w\text{-Fe}_h$  distances in **1** average  $2.52\text{ \AA}$ , and in **2**  $2.57\text{ \AA}$ , whereas in **3** the mean  $\text{Fe}_w\text{-Fe}_h$  distance is  $2.70\text{ \AA}$ . One point of similarity between **1**, **2** and **3** is the carbon-carbon bond length in the vinylidene fragment,  $1.44(1)\text{ \AA}$  for all three.

In several important details, the structures of **1** and **2** are quite similar to those of  $[\text{Fe}_4(\text{CO})_{12}\{\text{CC}(\text{O})(\text{OCH}_3)\}]^-$  and  $[\text{Fe}_4(\text{CO})_{12}\{\text{CC}(\text{O})(\text{CH}_3)\}]^-$ ,<sup>13</sup> even though the vinylidene ligands in **1** and **2** formally contain C=C double bonds while the C-C bond in the methylidyne clusters is formally a single bond. We previously described the structures of **1** and **2** on the basis of the orbital interactions between the  $\text{Fe}_4(\text{CO})_{12}$  butterfly unit and the  $\text{C}=\text{CR}^1\text{R}^2$  ( $\text{R}^1 = \text{OMe}$ ,  $\text{R}^2 = \text{OMe}$  or  $\text{Me}$ ) group.<sup>11</sup> The primary bonding interaction between the cluster core and the organic ligand involves overlap between the wingtip iron atoms and the  $\text{C} 2p_y$  orbital on the vinylidene carbon. (This  $2p_y$  orbital lies perpendicular to the plane of the vinylidene ligand and is thus oriented properly for  $\sigma$  interactions with the wingtip iron



Scheme 2



atoms and  $\pi$  interactions with the adjacent  $sp^2$ -hybridized C atom.) This cluster–ligand interaction, illustrated in structure **I**, is essentially the same as that by which the  $Fe_4(CO)_{12}$  core and the  $\mu_4$ -methylidyne ligands interact in the clusters  $[Fe_4(CO)_{12}\{CC(O)R\}]^-$  ( $R = Me$  or  $OMe$ ),<sup>18</sup> the principal difference being that the  $2p_y$  orbital on the vinylidene carbon is involved to a different degree with the adjacent  $sp^2$  vinyl carbon.

The methylidyne and vinylidene fragment orbitals which participate in the ligand–wingtip iron bonding interaction shown in structure **I** in  $[Fe_4(CO)_{12}\{CC(O)(OCH_3)\}]^-$ ,  $[Fe_4(CO)_{12}\{CC(O)(CH_3)\}]^-$ , **1**, **2** and **3** are illustrated in Fig. 2(a)–2(e), respectively. The coefficients of the relevant atomic orbitals are also shown for each fragment orbital. Comparisons of the diagrams and coefficients in Fig. 2(a) and 2(b) show that much of the electron density in the methylidyne fragment orbitals is localized on the methylidyne carbon atom. Thus in the methylidyne clusters the ligand–wingtip iron interaction shown in **I** involves a carbon p lone pair type orbital. As we discussed previously,<sup>11</sup> the vinylidene fragment orbitals in **1** and **2** [Fig. 2(c) and 2(d)] show only a small shift in electron density away from the vinylidene carbon. This shift is larger in **2** than in **1** and reflects a small increase in the double bond character of the C–C bond. This increase can be correlated with the presence of one rather than two oxygen atoms in the vinylidene ligand in **2**, since as the number of oxygen atoms decreases, the number of electrons available to participate in the  $\pi$  framework of the vinylidene group decreases and the  $\pi$  bonding framework becomes more localized between the two carbon atoms.

These results showed that even though the ligands in both **1**

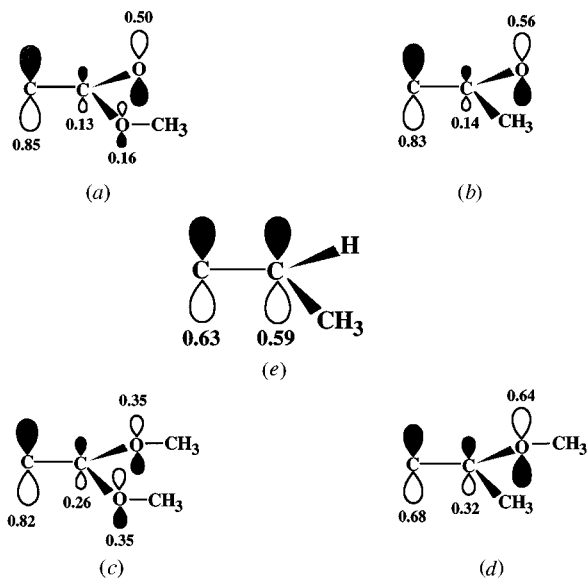
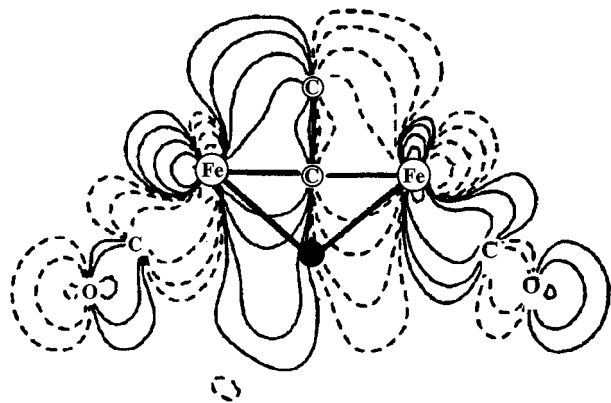


Fig. 2 Schematic representations of the orbitals on the methylidyne and vinylidene fragments, (a)  $[CC(O)OCH_3]^-$ , (b)  $[CC(O)CH_3]^-$ , (c)  $CC(OCH_3)_2$ , (d)  $CC(OCH_3)CH_3$  and (e)  $CC(H)CH_3$ , which interact with the wingtip iron atoms in each of the corresponding clusters. The coefficients of the atomic orbitals are indicated in each diagram

and **2** are viewed as formally incorporating C–C double bonds, the bonds in fact exhibit only partial double bond character. The orbital structures of these ligands provide an explanation for the similar structures of the methylidyne clusters and the vinylidene clusters **1** and **2**. The carbon  $2p_y$  orbital on the vinylidene carbon atom in cluster **1** is equally as available for cluster bonding as it is in the methylidyne cluster  $[Fe_4(CO)_{12}\{CC(O)(OCH_3)\}]^-$ ,<sup>18</sup> and the carbon–carbon bond in the vinylidene is virtually the same as that in the methylidyne cluster. This is evidenced by the vinylidene C=C bond length in **1**, which is only 0.05 Å shorter than the C–C bond in  $[Fe_4(CO)_{12}\{CC(O)(OCH_3)\}]^-$ . In **2**, however, the carbon  $2p_y$  orbital is more involved in a  $\pi$  interaction with the adjacent  $sp^2$  carbon in the vinylidene group, p electron density shifts slightly away from the vinylidene carbon, and the carbon–carbon bond begins to take on somewhat more double-bond character. Since the only bonding interaction between the wingtip iron atoms and the vinylidene group involves electrons which occupy the vinylidene  $\pi$  orbital, the cluster framework closes up around the vinylidene group to gain access to these electrons; this closing of the dihedral angle is compensated by a slight lengthening of the  $Fe_w$ – $Fe_h$  bonds. The decrease in the dihedral angle can thus be related to an increase in double-bond character in the vinylidene ligand.

Taken in this context, the character of the vinylidene  $\pi$  fragment orbital for cluster **3** [Fig. 2(e)] provides an explanation for the structure of **3**. When there are no oxygen atoms present in the vinylidene ligand there is a significant shift of p electron density away from the vinylidene carbon. The carbon–carbon bond becomes a true double bond, and the electrons needed for bonding with the wingtip iron atoms are now shared nearly equally between the two carbon atoms. As was seen for **2**, as the necessary electron density shifts away from the vinylidene carbon the cluster compensates by closing the dihedral angle and lengthening the  $Fe_w$ – $Fe_h$  bonds. The changes in both dihedral angle ( $104^\circ$  in **3** versus  $127^\circ$  in **2**), and  $Fe_w$ – $Fe_h$  bond lengths (2.70 Å in **3** versus 2.57 Å in **2**) are much larger for **3** and reflect the pronounced shift of electron density away from the vinylidene carbon. The cluster must now close around the C–C double bond in order for the wingtip iron atoms to bond with the vinylidene ligand. An orbital contour plot of the resulting cluster molecular orbital is shown in Fig. 3. The plot, which shows the plane occupied by the two wingtip iron atoms,



**Fig. 3** Contour plot showing the interaction in cluster **3** between the double bond of the vinylidene and the wingtip carbon atoms. The plot is in the plane defined by the two wingtip irons and the vinylidene carbon atom

the vinylidene carbon atom, and the midpoint of the  $\text{Fe}_h\text{-Fe}_h$  bond, illustrates that bonding between the vinylidene fragment and the wingtip iron atoms now involves the electron density in the C-C  $\pi$  bond rather than electron density in a vinylidene carbon p lone-pair orbital.

It should be noted that even though we can formally view the C-C bond in **3** as a double bond, the actual C-C bond length in **3** [1.441(8) Å] is no shorter than in **1** or **2**. This reflects the fact that the vinylidene ligand is not an isolated entity but is instead part of the overall cluster. In **3**, for example, the electrons which occupy the vinylidene p bonding orbital are now incorporated into a delocalized cluster orbital. This decreases (in the cluster) the electron density between the two carbon atoms and precludes shortening of the C-C bond.

## Conclusion

The synthesis and the molecular and electronic structure of the  $\mu_4$ -vinylidene tetrairon butterfly cluster,  $\text{Fe}_4(\text{CO})_{12}(\text{C}=\text{CHCH}_3)$  **3**, have been described. The cluster has an open butterfly framework of four iron atoms with a vinylidene ligand bound to all four metal atoms; the vinylidene ligand is approximately coplanar with the two hinge iron atoms. The  $\text{Fe}_4\text{C}$  core of the cluster is similar in structure to the  $\text{Fe}_4\text{C}$  cores of the previously reported vinylidene clusters  $\text{Fe}_4(\text{CO})_{12}[\text{C}=\text{C}(\text{OCH}_3)_2]$  **1** and  $\text{Fe}_4(\text{CO})_{12}[\text{C}=\text{C}(\text{CH}_3)(\text{OCH}_3)]$  **2**. The major differences in the structure of **3** are found in the dihedral angle between the wings of the butterfly and the position of the vinylidene carbon atom with respect to the wingtip iron atoms. The dihedral angle is considerably smaller in **3** than in **1** or **2**, and the butterfly actually closes around the vinylidene ligand to the extent that the vinylidene carbon atom lies below the vector connecting the two wingtip iron atoms. This is in marked contrast to the structures of all the previously characterized iron butterfly clusters. The closing of the butterfly dihedral angle is also accompanied by an increase in the length of the  $\text{Fe}_w\text{-Fe}_h$  bonds. As was found in **1** and **2**, the disposition of the CO ligands is much less symmetric than in their methylidyne analogs. This reorientation of the CO ligands appears to be dictated by steric crowding which results from the bulkiness of the substituents on the vinylidene ligand combined with the smaller dihedral angle between the two wings of the butterfly.

The changes in core geometry can be attributed to the electronic structure of the vinylidene ligand. Although clusters **1**, **2** and **3** all formally contain a C-C double bond in the vinylidene ligand, a true localized double bond occurs only in **3**. The oxygen atoms in the ligands in **1** and **2** lead to delocalized  $\pi$  systems and only partial double-bond character in the C-C bonds in these clusters. Although the double-bond character increases as the number of oxygen atoms incorporated into the ligand

decreases, a localized C-C double bond is found only in **3**, where no oxygen atoms occur in the ligand. Changes in the structure of the cluster framework in **3** can be related to the true double-bond character in the vinylidene ligand. While the formation of this double bond is accompanied by a marked shift in electron density away from the vinylidene carbon atom, these ligand p electrons must also participate in bonding with the wingtip iron atoms. The cluster closes up around the vinylidene to gain access to this electron density.

## Experimental

All preparative procedures were performed in standard Schlenk glassware on a double-manifold vacuum-nitrogen line. The starting material  $\text{Fe}_4(\text{CO})_{12}[\text{C}=\text{C}(\text{OCH}_3)(\text{CH}_3)]$  **2** was prepared by methylation of  $[\text{NET}_4]^+[\text{Fe}_4(\text{CO})_{12}\{\text{CC}(\text{O})(\text{CH}_3)\}]^-$ <sup>19</sup> with trimethylxonium fluoroborate as previously described.<sup>11</sup> Lithium triethylhydroborate (1.0 M tetrahydrofuran solution) and trimethylsilyl trifluoromethanesulfonate were used as supplied by Aldrich. Infrared spectra were recorded on a Mattson Galaxy 5000 FT-IR spectrometer in dichloromethane solutions using  $\text{CaF}_2$  sealed solution cells, or as KBr pellets.

### Preparation of $\text{Fe}_4(\text{CO})_{12}(\text{C}=\text{CHCH}_3)$ , **3**

To a solution of **2** (0.475 g, 0.74 mmol) in tetrahydrofuran at  $-78^\circ\text{C}$  was added a solution of lithium triethylhydroborate (0.75 cm<sup>3</sup> of a 1.0 M thf solution). The initially brown solution turned deep green. The IR spectrum of the solution, taken in a precooled ( $-78^\circ\text{C}$ ) cell, showed principal absorbances characteristic of monoanionic  $\text{Fe}_4\text{C-X}$  butterfly clusters at 2000s and 1974 cm<sup>-1</sup>. To the cold reaction mixture was added trimethylsilyl trifluoromethanesulfonate (0.17 g, 0.74 mmol), and the solution became brown in color. The solvent was removed under reduced pressure and the residue extracted into pentane at room temperature. On cooling the pentane extracts to  $-78^\circ\text{C}$  black crystals separated, and these were collected by filtration at this temperature. Recrystallization from hexane at  $-78^\circ\text{C}$  yielded **3** as a black crystalline solid. Yield 0.167 g, 0.28 mmol, 37.5% (Found: C, 29.95; H, 0.62; Fe, 36.98. Calc. for  $\text{C}_{15}\text{H}_4\text{Fe}_4\text{O}_{12}$ : C, 30.05; H, 0.67; Fe, 37.26%). IR(hexane)/cm<sup>-1</sup>: 2098w, 2058s, 2030s, 1980m. <sup>13</sup>C NMR (100 MHz,  $\text{CD}_2\text{Cl}_2$ ,  $25^\circ\text{C}$ ):  $\delta$  213.5 [3 C,  $\text{Fe}_h(\text{CO})_3$ ], 213.1 [3 C,  $\text{Fe}_h(\text{CO})_3$ ], 206.8 [6 C,  $\text{Fe}_w(\text{CO})_3$ ]. Resonances due to the vinylidene carbons C(13) and C(14) were not located.

### X-Ray crystallography

The crystal structure of  $\text{Fe}_4(\text{CO})_{12}(\mu_4\text{-}\eta^2\text{-C}=\text{CHCH}_3)$  **3** was determined at Crystalytics Inc., Lincoln, NE. Details of data collection and structure refinement are given in Table 1. Crystals of **3** were grown from hexane solution at  $-40^\circ\text{C}$ . Data were collected on a crystal sealed under nitrogen in a capillary, on a four-circle Nicolet Autodiffractometer. The intensities of six check reflections were monitored throughout data collection and no decay was evident. Of 3303 independent reflections collected ( $3 < 2\theta < 48^\circ$ ) 1986 with  $I > 3\sigma(I)$  were used in structure solution and refinement. Data were corrected empirically for absorption effects using  $\psi$  scans for seven reflections having  $2\theta$  between  $7.78$  and  $34.1^\circ$  ( $\mu = 27.9$  cm<sup>-1</sup>,<sup>21</sup> maximum, minimum transmission factors 0.453, 1.000), and then reduced to relative squared amplitudes,  $|F_o|^2$ , by means of standard Lorentz and polarisation corrections.

The structure solutions were carried out on a Data-General Eclipse S-200 computer using SHELXTL<sup>22</sup> interactive crystallographic software as modified at Crystalytics Company. The thirty-one non-hydrogen atoms were located using direct methods (SHELXTL). Hydrogen atoms were located by Fourier-difference synthesis. Least-squares refinement was carried out converging to final residuals  $R^1 = 0.043$ ,  $R^2 = 0.041$  ( $R^1$  and  $R^2$  being defined as in Table 1). The non-hydrogen

**Table 1** Crystal data for Fe<sub>4</sub>(CO)<sub>12</sub>(C=CHCH<sub>3</sub>)

Formula	C <sub>15</sub> H <sub>4</sub> Fe <sub>4</sub> O <sub>12</sub>
<i>M</i>	599.6
Crystal system	<i>Pbca</i> ( <i>D</i> <sup>15</sup> 2h, no. 61) <sup>20</sup>
<i>a</i> /Å	16.694(6)
<i>b</i> /Å	14.882(6)
<i>c</i> /Å	16.741(6)
<i>U</i> /Å <sup>3</sup>	4159(2)
<i>Z</i>	8
Crystal dimensions/mm	0.55 × 0.55 × 0.55
Color	Black
<i>D</i> <sub>c</sub> /g cm <sup>-3</sup>	1.92
Reflections collected	3303
Independent reflections	3303
Independent reflections observed	1986
Variation in check reflections	<1%
<i>R</i> <sub>1</sub> <sup>a</sup>	0.043
<i>R</i> <sub>2</sub> <sup>b</sup>	0.041
Residual electron density/e Å <sup>-3</sup>	<0.47 (background noise level)
<i>N</i> <sub>o</sub> / <i>N</i> <sub>v</sub>	7

<sup>a</sup>  $R^1 = \sum ||F_o| - |F_c|| / \sum |F_o|$ . <sup>b</sup>  $R^2 = [\sum w(|F_o| - |F_c|)^2 / \sum w|F_o|^2]^{1/2}$ . <sup>c</sup> Weighting scheme  $w = 1/\sigma_F^2$  ( $\sigma_F = \{[\sigma(F_o)]^2 + 0.01(|F_o|)^2\}^{1/2}$ ). *N*<sub>o</sub> = Number of observed independent reflections, *N*<sub>v</sub> = number of refined parameters.

**Table 2** Selected interatomic distances (Å) and bond angles for Fe<sub>4</sub>(CO)<sub>12</sub>(C=CHCH<sub>3</sub>)

Fe(1)–Fe(2)	2.668(1)	Fe(1)–Fe(3)	2.669(1)
Fe(1)–Fe(4)	2.544(1)	Fe(2)–Fe(4)	2.730(2)
Fe(3)–Fe(4)	2.711(1)	Fe(2)–C(13)	1.867(7)
Fe(1)–C(13)	1.922(6)	Fe(4)–C(13)	1.875(6)
Fe(3)–C(13)	1.872(7)	C(14)–C(15)	1.504(10)
C(13)–C(14)	1.441(8)	Fe(3)⋯C(15)	2.321(7)
Fe(2)⋯C(15)	2.320(7)		
Fe(2)–Fe(2)–Fe(3)	88.8(1)	Fe(2)–Fe(1)–Fe(4)	63.1(1)
Fe(3)–Fe(1)–Fe(4)	62.6(1)	Fe(1)–Fe(2)–Fe(4)	56.2(1)
Fe(1)–Fe(3)–Fe(4)	56.4(1)	Fe(1)–Fe(4)–Fe(2)	60.7(1)
Fe(1)–Fe(4)–Fe(3)	60.9(1)	Fe(2)–Fe(4)–Fe(3)	86.6(1)
Fe(2)–C(13)–Fe(3)	173.4(3)	Fe(3)–C(13)–Fe(4)	92.7(3)
Fe(2)–C(13)–C(14)	88.0(3)	Fe(3)–C(13)–C(14)	88.0(3)
Fe(1)–C(13)–C(14)	133.4(3)	Fe(4)–C(13)–C(14)	142.5(3)
C(13)–C(14)–C(15)	127.2(6)	C(13)–C(14)–H	114(3)

atoms were refined anisotropically, and anomalous dispersion factors for the iron atoms were taken from the literature.<sup>21</sup>

CCDC reference number 186/604.

Selected bond lengths and angles discussed in the text are given in Table 2. The atom numbering scheme used is shown in the ORTEP drawing of the molecule (Fig. 1) in which the non-hydrogen atoms are represented as thermal ellipsoids encompassing 50% of their electron density. Hydrogen atoms are represented by small spheres of arbitrary radius.

### Molecular orbital calculations

Molecular orbital calculations using the Fenske–Hall method<sup>23</sup> were carried out for Fe<sub>4</sub>(CO)<sub>12</sub>(C=CHCH<sub>3</sub>) **3**. Calculations for [Fe<sub>4</sub>(CO)<sub>12</sub>(CCO<sub>2</sub>CH<sub>3</sub>)]<sup>-</sup>, [Fe<sub>4</sub>(CO)<sub>12</sub>{CC(O)CH<sub>3</sub>}]<sup>-</sup>, Fe<sub>4</sub>(CO)<sub>12</sub>[C=C(OCH<sub>3</sub>)<sub>2</sub>] **1** and Fe<sub>4</sub>(CO)<sub>12</sub>[C=C(CH<sub>3</sub>)(OCH<sub>3</sub>)] **2**, have been reported previously,<sup>11,13</sup> and the results of those calculations are used for comparison here. Atomic positions used in the calcu-

lations for **3** were taken from the crystal structure reported here. The 1s through 3d functions for Fe were taken from Richardson *et al.*,<sup>24</sup> while the 4s and 4p were chosen to have exponents of 2.0. The carbon and oxygen functions were taken from the double- $\zeta$  functions of Clementi.<sup>25</sup> The valence 2p functions were retained as the double- $\zeta$  functions, while the 1s and 2s functions were reduced to single- $\zeta$  form. An exponent of 1.2 was used for hydrogen. In all of the calculations the local coordinate system on the vinylidene carbon was oriented with the *x* axis parallel to a line connecting the two hinge iron atoms Fe(1) and Fe(4), the *y* axis parallel to a line connecting the two wingtip iron atoms, Fe(2) and Fe(3), and the *z* axis pointing out of the cluster.

### References

- E. Sappa, A. Tiripicchio and M. Tiripicchio Camellini, *Inorg. Chim. Acta*, 1980, **41**, 11.
- A. J. Carty, S. A. MacLaughlin and N. J. Taylor, *J. Chem. Soc., Chem. Commun.*, 1981, 476.
- P. Brun, G. M. Dawkins, M. Green, R. M. Mills, J.-Y. Salaün, F. G. A. Stone, and P. Woodward, *J. Chem. Soc., Dalton Trans.*, 1983, 1357.
- A. J. Carty, N. J. Taylor, E. Sappa and A. Tiripicchio, *Inorg. Chem.*, 1983, **22**, 1871.
- E. Sappa, A. Tiripicchio and M. Tiripicchio Camellini, *J. Organomet. Chem.*, 1983, **246**, 287.
- J. C. Jeffrey, B. F. G. Johnson, J. Lewis, P. R. Raithby and D. A. Welch, *J. Chem. Soc., Chem. Commun.*, 1986, 318.
- T. Albiez, A. K. Powell and H. Vahrenkamp, *Chem. Ber.*, 1990, **123**, 667.
- Y. Chi, S.-H. Chuang, L.-K. Liu and Y.-S. Wen, *Organometallics*, 1991, **10**, 2485.
- R. Rumin, F. Robin, F. Y. Pétillon, K. W. Muir and I. Stevenson, *Organometallics*, 1991, **10**, 2274.
- A. B. Antonova, A. A. Johansson, N. A. Deykhina, A. G. Ginzburg, E. D. Korniyets, S. V. Kovalenko, N. I. Pavlenko, P. V. Petrovskii, A. I. Rubaylo and I. A. Sukhina, *Inorg. Chim. Acta*, 1995, **230**, 97.
- J. S. Bradley, S. Harris, E. W. Hill and M. Modrick, *Polyhedron*, 1990, **9**, 1809.
- C. J. Adams, M. I. Bruce, B. W. Skelton and A. H. White, *J. Chem. Soc., Dalton Trans.*, 1992, 3057.
- J. S. Bradley, S. Harris, J. M. Newsam, E. W. Hill, S. Leta and M. Modrick, *Organometallics*, 1987, **6**, 2060.
- T. Kawasaki, Y. Nonaka, M. Kobayashi and M. Sakamoto, *J. Chem. Soc., Perkin Trans. 1*, 1991, 2445.
- M. Brookhardt and R. C. Buck, *J. Organomet. Chem.*, 1989, **370**, 111.
- J. R. Andrews, S. F. A. Kettle, D. B. Powell and N. Sheppard, *Inorg. Chem.*, 1982, **21**, 2874.
- C. K. Johnson, ORTEP, Report ORNL-5138, Oak Ridge National Laboratory, Oak Ridge, TN, 1976.
- S. Harris and J. S. Bradley, *Organometallics*, 1984, **3**, 1086.
- E. W. Hill and J. S. Bradley, *Inorg. Synth.*, 1989, **27**, 101.
- International Tables for X-Ray Crystallography*, Kynoch Press, Birmingham, 1969, vol. 1.
- International Tables for X-Ray Crystallography*, Kynoch Press, Birmingham, 1974, vol. 4.
- G. M. Sheldrick, SHELXTL, University of Göttingen, 1986.
- M. B. Hall and R. F. Fenske, *Inorg. Chem.*, 1972, **11**, 768.
- J. W. Richardson, W. C. Nieuvoort, R. R. Powell and W. F. Edgell, *J. Chem. Phys.*, 1962, **36**, 1507.
- E. Clementi, *J. Chem. Phys.*, 1964, **40**, 1944.

Received 19th May 1997; Paper 7/03418K